FERMILAB-PUB-17-379-E

Combined Forward-Backward Asymmetry Measurements in Top-Antitop Quark Production at the Tevatron

Supplemental Material

CDF and D0 Collaborations

In this document, we provide supplemental information on the combination of the CDF and D0 measurements of the forward-backward asymmetries in $t\bar{t}$ pair production at the Fermilab Tevatron [1].

I. $t\bar{t}$ PRODUCTION ASYMMETRY, $A_{\rm FB}^{t\bar{t}}$

Table I reports the uncertainties for each of the contributing measurements to the inclusive $t\bar{t}$ asymmetry, $A_{\rm FB}^{t\bar{t}}$, and the uncertainties for their combination in the fit. Table II shows the individual inclusive $A_{\rm FB}^{t\bar{t}}$ measurements and uncertainties, as well as their combination. The contribution, in terms of the weights determined by BLUE [2–4], of each measurement in the fit are also shown.

Table III shows the inputs to the differential $A_{\rm FB}^{t\bar{t}}$ vs. $m_{t\bar{t}}$ fit and their uncertainties. Figure 1 shows the combined result for the differential $A_{\rm FB}^{t\bar{t}}$ vs. $m_{t\bar{t}}$ data. The linear fit to the data and its one standard deviation (SD) uncertainty are shown by the black solid line and gray shaded band; the corresponding quantities for the theoretical prediction are shown by the orange line and shaded band. Figure 2 shows the correlations of the slope and intercept at $m_{t\bar{t}} = 450$ GeV/c^2 for the data and theoretical prediction. The smaller orange ellipse shows the correlation of the slope and intercept of the NNLO QCD + NLO EW prediction of Ref. [5–7].

Figure 3 shows the correlations of total uncertainties between adjacent $m_{t\bar{t}}$ bins, for the CDF and D0 data, as well as for the combination. The correlations between the individual CDF and D0 measurements for the third bin with adjacent bins of $m_{t\bar{t}}$ result in a combined asymmetry value that is smaller than either of the inputs for the third bin. This behavior indicates the presence of large correlations and can be understood when looking at the orientation of the correlation ellipses in Figure 3(c). The 68% confidence level ellipses show smaller uncertainties for the CDF inputs than for the D0 inputs. The smaller CDF uncertainties results from the different choice made by CDF for the regularization method used to correct for detector effects.

Table IV shows the covariance matrix of the combined differential $A_{\rm FB}^{t\bar{t}}$ vs. $m_{t\bar{t}}$. Table V shows the correlation matrix for the total uncertainties of the combined CDF and D0 differential $A_{\rm FB}^{t\bar{t}}$ vs. $m_{t\bar{t}}$. Table VI shows the inputs to the differential $A_{\rm FB}^{t\bar{t}}$ vs. $|\Delta y_{t\bar{t}}|$ fit and their uncertainties. Table VII shows the covariance matrix of the total uncertainties of the differential $A_{\rm FB}^{t\bar{t}}$ vs. $|\Delta y_{t\bar{t}}|$ inputs to the combined fit. Table VIII shows the correlation matrix of the total uncertainties of the differential $A_{\rm FB}^{t\bar{t}}$ vs. $|\Delta y_{t\bar{t}}|$ inputs.

II. SINGLE LEPTON ASYMMETRY, A^{ℓ}_{FB}

Table IX reports the uncertainties for each of the contributing measurements to the inclusive single lepton asymmetry, A^{ℓ}_{FB}, and the uncertainties for their combination in the fit. Table X shows the individual inclusive A^{ℓ}_{FB} measurements and uncertainties, as well as their combination. The weights of each measurement in the fit are also shown.

III. DILEPTON ASYMMETRY, $A^{\ell\ell}_{\mathrm{FB}}$

Table XI reports the uncertainties for each of the contributing measurements to the inclusive dilepton asymmetry $A^{\ell\ell}_{\mathrm{FB}}$ and the uncertainties for their combination in the fit. Table XII shows the individual inclusive $A^{\ell\ell}_{\mathrm{FB}}$ measurements and uncertainties, as well as their combination. The weights of each measurement in the fit are also shown.

Table I: Statistical and systematic uncertainties in the individual inclusive $A^{t\bar{t}}_{\mathrm{FB}}$ inputs as well as in the resultant combination.

Uncertainty	CDF ℓ+jets [8]	CDF $\ell\ell$ [9]	D0 ℓ+jets [10]	D0 $\ell\ell$ [11]	Combination
Statistical	0.039	0.11	0.027	0.056	0.021
Background	0.022	0.04	0.010	0.007	0.008
Signal	0.011	0.05	0.005	0.026	0.009
Detector	0.007	0.02	0.003	0.001	0.003
Method	0.004	0.02	0.005	0.014	0.004
PDF	0.001	0.01	0.004	0.003	0.003

Table II: Inputs to the combination of the inclusive $t\bar{t}$ asymmetries and results of the combination.

Analysis	$A^{t\bar{t}}_{\mathrm{FB}}$	Uncertainty			Weight
		Stat.	Syst.	Total	
CDF ℓ+jets [8]	0.164	0.039	0.026	0.047	0.25
CDF $\ell\ell$ [9]	0.12	0.11	0.07	0.13	0.01
D0 ℓ+jets [10]	0.106	0.027	0.013	0.030	0.64
D0 $\ell\ell$ [11]	0.175	0.056	0.031	0.063	0.11
Combination	0.128	0.021	0.014	0.025	

Table III: Inputs of the $A_{\rm FB}^{t\bar{t}}$ results in the ℓ+jets channels, along with their statistical (Stat) and systematic uncertainties broken down for the individual $m_{t\bar{t}}$ bins. The listed systematic uncertainties originate from the measurement method (Method), signal modeling (Signal), parton-distribution function (PDF), detector modeling (Detector), and from background shape (Bkd dist) and background normalization (Bkd norm).

$m_{t\bar{t}}$ [GeV/c^2]	$A_{\rm FB}^{t\bar{t}}$	Uncertainty							
		Total	Stat	Method	Signal	PDF	Detector	Bkd dist	Bkd norm
D0 ℓ+jets									
350–450	0.079	0.050	0.046	0.011	0.015	0.005	0.005	0.007	0.001
450–550	0.141	0.064	0.060	0.018	0.010	0.011	0.0024	0.007	0.001
550–650	0.376	0.188	0.181	0.011	0.028	0.035	0.018	0.010	0.002
> 650	-0.123	0.292	0.287	0.017	0.009	0.043	0.030	0.014	0.003
CDF ℓ+jets									
350–450	0.084	0.055	0.046	0.012	0.009	0.001	0.013	0.021	0.008
450–550	0.255	0.071	0.062	0.002	0.021	0.001	0.013	0.017	0.016
550–650	0.370	0.121	0.084	0.001	0.077	0.001	0.032	0.011	0.021
> 650	0.493	0.193	0.158	0.023	0.091	0.001	0.045	0.021	0.031

Table IV: Covariance matrix of the combined CDF and D0 differential $A_{\rm FB}^{t\bar{t}}$ vs. $m_{t\bar{t}}$.

$m_{t\bar{t}}$ [GeV/c^2]	350–450	450–550	550–650	> 650
350–450	$+0.0013690$	$+0.0007672$	$+0.0002512$	$+0.0003644$
450–550	$+0.0007672$	$+0.0023040$	$+0.0012140$	-0.0005292
550–650	$+0.0002512$	$+0.0012140$	$+0.0086490$	$+0.0057140$
> 650	$+0.0003644$	-0.0005292	$+0.0057140$	$+0.0216100$

Table V: Correlation matrix for the total uncertainties of the combined CDF and D0 differential $A_{\rm FB}^{t\bar{t}}$ vs. $m_{t\bar{t}}$.

$m_{t\bar{t}}$ [GeV/c^2]	$350-450$	$450-550$	$550-650$	> 650
$350-450$	$+1.000$	$+0.432$	$+0.073$	$+0.067$
$450-550$	$+0.432$	$+1.000$	$+0.272$	-0.075
$550-650$	$+0.073$	$+0.272$	$+1.000$	$+0.418$
> 650	$+0.067$	-0.075	$+0.418$	$+1.000$

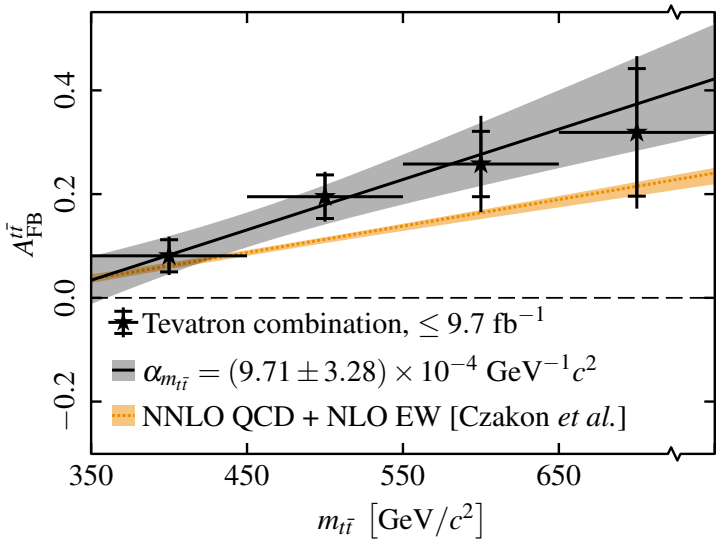

Figure 1: Differential $A_{\mathrm{FB}}^{t\bar{t}}$ vs. $m_{t\bar{t}}$ for the Tevatron combination. The linear slope of the combined result is given by the solid black line together with the total uncertainty of the two-parameter fit (shaded gray area). The dashed solid orange line shows the NNLO QCD + NLO EW prediction of Refs. [5–7], while the shaded orange area shows the 1 SD theoretical uncertainty on the prediction.

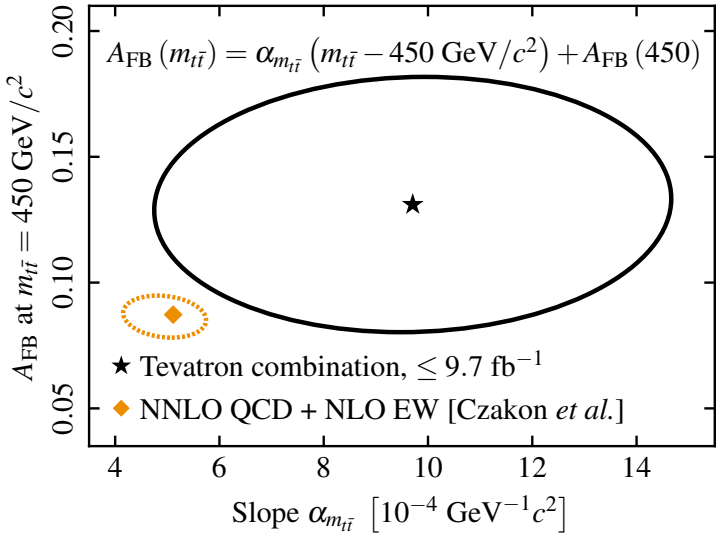

Figure 2: Correlation of the slope and intercept from the linear fit of the $A_{\mathrm{FB}}^{t\bar{t}}$ vs. $m_{t\bar{t}}$ data represented as 68% confidence ellipses, and shown at $m_{t\bar{t}} = 450$ GeV/c^2. The smaller dashed orange ellipse shows the correlation of the slope and intercept of the NNLO QCD + NLO EW prediction of Refs. [5–7].

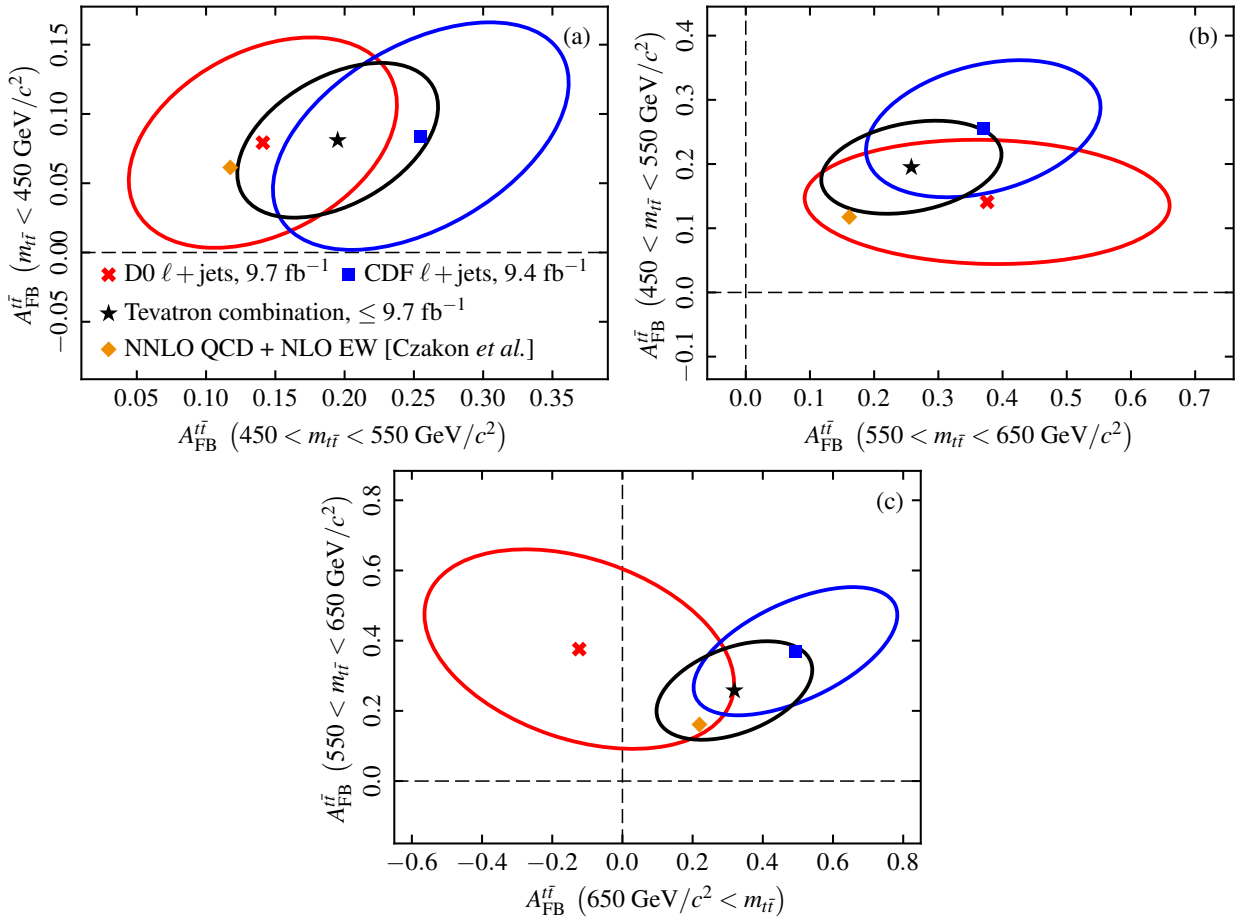

Figure 3: Correlations of combined statistical and systematic uncertainties represented as 68% confidence ellipses between the first and second $A_{\rm FB}^{t\bar{t}}$ vs. $m_{t\bar{t}}$ bin (a), the second and third $A_{\rm FB}^{t\bar{t}}$ vs. $m_{t\bar{t}}$ bin (b), and the third and fourth $A_{\rm FB}^{t\bar{t}}$ vs. $m_{t\bar{t}}$ bin (c). The orange marker shows the NNLO QCD + NLO EW theoretical prediction [5–7] while the dashed orange ellipse shows the theoretical uncertainty on the prediction.

Table VI: Inputs of the differential $A_{\rm FB}^{t\bar{t}}$ vs. $|\Delta y_{t\bar{t}}|$ results in the ℓ+jets channels and $\ell\ell$ channel. Their statistical and systematic uncertainties are broken down for the individual $|\Delta y_{t\bar{t}}|$ bins. The listed systematic uncertainties originate from the measurement method (Method), signal modeling (Signal), parton-distribution function (PDF), detector modeling (Detector), and from background shape (Bkd dist) and background normalization (Bkd norm).

$\Delta y_{t\bar{t}}$	$A_{\rm FB}^{t\bar{t}}$	Uncertainty							
		Total	Statistical	Method	Signal	PDF	Detector	Bkd dist	Bkd norm
D0 ℓ+jets									
0.00–0.25	0.018	0.012	0.010	0.004	0.004	0.002	0.003	0.004	0.001
0.25–0.50	0.054	0.033	0.029	0.009	0.008	0.003	0.005	0.008	0.001
0.50–1.00	0.108	0.048	0.045	0.010	0.009	0.004	0.006	0.009	0.001
> 1.00	0.218	0.071	0.064	0.017	0.015	0.007	0.010	0.016	0.002
CDF ℓ+jets									
0.00–0.50	0.048	0.042	0.034	0.004	0.017	0.001	0.005	0.017	0.005
0.50–1.00	0.180	0.074	0.057	0.008	0.027	0.001	0.015	0.029	0.017
1.00–1.50	0.356	0.088	0.080	0.001	0.013	0.001	0.004	0.005	0.032
> 1.50	0.477	0.151	0.132	0.018	0.034	0.004	0.012	0.044	0.043
CDF $\ell\ell$									
0.00–0.50	0.12	0.39	0.33	0.06	0.16	0.01	0.02	0.13	
> 0.50	0.13	0.17	0.13	0.02	0.09	0.01	0.02	0.06	

Table VII: Covariance matrix of the statistical and systematic uncertainties of the differential $A_{\rm FB}^{t\bar{t}}$ vs. $|\Delta y_{t\bar{t}}|$ results employed in the combined χ^2 fit. The PDF and signal uncertainties are assumed to be fully correlated between CDF and D0 (+1), while others are assumed to be uncorrelated.

	D0 ℓ+jets				CDF ℓ+jets				CDF $\ell\ell$	
$\Delta y_{t\bar{t}}$	0.00–0.25	0.25–0.50	0.50–1.00	> 1.00	0.00–0.50	0.50–1.00	1.00–1.50	> 1.50	0.00–0.50	> 0.50
D0 ℓ+jets										
0.00–0.25	+1.5590e-04	+3.1260e-04	+4.3580e-04	+2.0598e-04	+6.7363e-05	+1.0965e-04	+5.4530e-05	+1.4314e-04	+6.1059e-04	+3.8000e-04
0.25–0.50	+3.1260e-04	+1.0914e-03	+1.3690e-03	+5.2010e-04	+1.3438e-04	+2.1827e-04	+1.0809e-04	+2.8259e-04	+1.2112e-03	+7.5000e-04
0.50–1.00	+4.3580e-04	+1.3690e-03	+2.3518e-03	+1.1144e-03	+1.5107e-04	+2.4518e-04	+1.2126e-04	+3.1653e-04	+1.3588e-03	+8.4000e-04
> 1.00	+2.0598e-04	+5.2010e-04	+1.1144e-03	+4.9802e-03	+2.5234e-04	+4.1067e-04	+2.0392e-04	+5.3492e-04	+2.2847e-03	+1.4200e-03
CDF ℓ+jets										
0.00–0.50	+6.7363e-05	+1.3438e-04	+1.5107e-04	+2.5234e-04	+1.7632e-03	+2.0343e-03	+2.0723e-05	−2.0149e-03	+2.5367e-03	−1.3013e-03
0.50–1.00	+1.0965e-04	+2.1827e-04	+2.4518e-04	+4.1067e-04	+2.0343e-03	+5.3518e-03	+2.4451e-03	−2.7678e-04	−1.4144e-04	+1.1556e-04
1.00–1.50	+5.4530e-05	+1.0809e-04	+1.2126e-04	+2.0392e-04	+2.0723e-05	+2.4451e-03	+7.6970e-03	+1.1443e-02	−5.2223e-04	+6.4377e-04
> 1.50	1.4314e-04	+2.8259e-04	+3.1653e-04	+5.3492e-04	−2.0149e-03	−2.7678e-04	+1.1443e-02	+2.2995e-02	−3.0824e-03	+2.6086e-03
CDF $\ell\ell$										
0.00–0.50	+6.1059e-04	+1.2112e-03	+1.3588e-03	+2.2847e-03	+2.5367e-03	−1.4144e-04	−5.2223e-04	−3.0824e-03	+1.5170e-01	−2.2280e-02
> 0.50	+3.8000e-04	+7.5000e-04	+8.4000e-04	+1.4200e-03	−1.3013e-03	+1.1556e-04	+6.4377e-04	+2.6086e-03	−2.2280e-02	+2.9500e-02

Table VIII: Correlation matrix of the total uncertainties of the differential $A_{\rm FB}^{t\bar{t}}$ vs. $|\Delta y_{t\bar{t}}|$ results employed in the combined χ^2 fit. The PDF and signal uncertainties are assumed to be fully correlated between CDF and D0 (+1), while others are assumed to be uncorrelated.

	D0 ℓ+jets				CDF ℓ+jets				CDF $\ell\ell$	
$\Delta y_{t\bar{t}}$	0.00–0.25	0.25–0.50	0.50–1.00	> 1.00	0.00–0.50	0.50–1.00	1.00–1.50	> 1.50	0.00–0.50	> 0.50
D0 ℓ+jets										
0.00–0.25	+1.000	+0.758	+0.720	+0.234	+0.128	+0.120	+0.050	+0.076	+0.126	+0.177
0.25–0.50	+0.758	+1.000	+0.854	+0.223	+0.097	+0.090	+0.037	+0.056	+0.094	+0.132
0.50–1.00	+0.720	+0.854	+1.000	+0.326	+0.074	+0.069	+0.029	+0.043	+0.072	+0.101
> 1.00	+0.234	+0.223	+0.326	+1.000	+0.085	+0.080	+0.033	+0.050	+0.083	+0.117
CDF ℓ+jets										
0.00–0.50	+0.128	+0.097	+0.074	+0.085	+1.000	+0.662	+0.006	−0.316	+0.155	−0.180
0.50–1.00	+0.120	+0.090	+0.069	+0.080	+0.662	+1.000	+0.381	−0.025	−0.005	+0.009
1.00–1.50	+0.050	+0.037	+0.029	+0.033	+0.006	+0.381	+1.000	+0.860	−0.015	+0.043
> 1.50	+0.076	+0.056	+0.043	+0.050	−0.316	−0.025	+0.860	+1.000	−0.052	+0.100
CDF $\ell\ell$										
0.00–0.50	+0.126	+0.094	+0.072	+0.083	+0.155	−0.005	−0.015	−0.052	+1.000	−0.333
> 0.50	+0.177	+0.132	+0.101	+0.117	−0.180	+0.009	+0.043	+0.100	−0.333	+1.000

Table IX: Statistical and systematic uncertainties in the individual inclusive $A_{\rm FB}^{\ell}$ inputs.

Uncertainty	CDF ℓ+jets [12]	CDF $\ell\ell$ [13]	D0 ℓ+jets [14]	D0 $\ell\ell$ [15]	Combination
Statistical	0.024	0.052	0.027	0.037	0.016
Background	0.015	0.029	$^{+0.016}_{-0.018}$	0.008	0.008
Signal	0.007	< 0.001	0.008	0.005	0.006
Detector	0.002	0.004	$^{+0.008}_{-0.011}$	0.005	0.004
Method	$^{+0.013}_{-0.000}$	0.006	0.008	0.004	0.005
PDF	0.003	< 0.001	0.002	< 0.001	0.002

Table X: Inputs to and results from the combination of the inclusive $A_{\rm FB}^{\ell}$ asymmetries.

Analysis	$A_{\rm FB}^{\ell}$	Uncertainty			Weight
		Stat.	Syst.	Total	
CDF ℓ+jets [12]	0.105	0.024	$^{+0.022}_{-0.017}$	$^{+0.032}_{-0.029}$	0.40
CDF $\ell\ell$ [13]	0.072	0.052	0.030	0.060	0.11
D0 ℓ+jets [14]	0.050	0.027	$^{+0.020}_{-0.024}$	$^{+0.034}_{-0.037}$	0.27
D0 $\ell\ell$ [15]	0.044	0.037	0.011	0.039	0.23
Combination	0.073	0.016	0.012	0.020	

Table XI: Statistical and systematic uncertainties in the individual inclusive $A_{\rm FB}^{\ell\ell}$ inputs as well as in the combined results.

Uncertainty	CDF $\ell\ell$ [13]	D0 $\ell\ell$ [15]	Combination
Statistical	0.072	0.054	0.043
Background	0.037	0.009	0.013
Signal	< 0.001	0.009	0.001
Detector	0.003	0.006	0.008
Method	0.013	0.004	0.005
PDF	< 0.001	< 0.001	0.001

Table XII: Inputs to and results from the combination of the inclusive $A_{\rm FB}^{\ell\ell}$ asymmetries.

Analysis	$A_{\rm FB}^{\ell\ell}$	Uncertainty			Weight
		Stat.	Syst.	Total	
CDF $\ell\ell$ [13]	0.076	0.072	0.037	0.082	0.32
D0 $\ell\ell$ [15]	0.123	0.054	0.015	0.056	0.68
Combination	0.108	0.043	0.016	0.046	

[1] T. Aaltonen *et al.* (CDF and D0 Collaboration), Combined Forward-Backward Asymmetry Measurements in Top-Antitop Quark Production at the Tevatron, submitted to Phys. Rev. Lett. (2017).

[2] L. Lyons, D. Gibaut, and P. Clifford, How to combine correlated estimates of a single physical quantity, Nucl. Instrum. Methods Phys. Res., Sect. A **270**, 110 (1988).

[3] L. Lyons, A.J. Martin, and D.H. Saxon, On the determination of the B lifetime by combining the results of different experiments, Phys. Rev. D **41**, 982 (1990).

[4] A. Valassi, Combining correlated measurements of several different physical quantities, Nucl. Instrum. Methods Phys. Res., Sect. A **500**, 391 (2003).

[5] M. Czakon, P. Fiedler, D. Heymes, and A. Mitov, NNLO QCD predictions for fully-differential top-quark pair production at the Tevatron, J. High Energy Phys. 05 (2016) 034.

[6] M. Czakon, P. Fiedler, and A. Mitov, Resolving the Tevatron Top Quark Forward-Backward Asymmetry Puzzle: Fully Differential Next-to-Next-to-Leading-Order Calculation, Phys. Rev. Lett. **115**, 052001 (2015).

[7] M. Czakon, D. Heymes, A. Mitov, D. Pagani, I. Tsinikos, and M. Zaro, Top-pair production at the LHC through NNLO QCD and NLO EW, [arXiv:1705.04105] (2017).

[8] T. Aaltonen *et al.* (CDF Collaboration), Measurement of the top quark forward-backward production asymmetry and its dependence on event kinematic properties, Phys. Rev. D **87**, 092002 (2013).

[9] T. Aaltonen *et al.* (CDF Collaboration), Measurement of the forward-backward asymmetry of top-quark and antiquark pairs using the full CDF Run II data set, Phys. Rev. D **93**, 112005 (2016).

[10] V.M. Abazov *et al.* (D0 Collaboration), Measurement of the forward-backward asymmetry in top quark-antiquark production in $p\bar{p}$ collisions using the lepton+jets channel, Phys. Rev. D **90**, 072011 (2014).

[11] V.M. Abazov *et al.* (D0 Collaboration), Simultaneous measurement of forward-backward asymmetry and top polarization in dilepton final states from $t\bar{t}$ production at the Tevatron, Phys. Rev. D **92**, 052007 (2015).

[12] T. Aaltonen *et al.* (CDF Collaboration), Measurement of the leptonic asymmetry in $t\bar{t}$ events produced in $p\bar{p}$ collisions at $\sqrt{s} = 1.96$ TeV, Phys. Rev. D **88**, 072003 (2013).

[13] T. Aaltonen *et al.* (CDF Collaboration), Measurement of the Inclusive Leptonic Asymmetry in Top-Quark Pairs that Decay to Two Charged Leptons at CDF, Phys. Rev. Lett. **113**, 042001 (2014).

[14] V.M. Abazov *et al.* (D0 Collaboration), Measurement of the forward-backward asymmetry in the distribution of leptons in $t\bar{t}$ events in the lepton+jets channel, Phys. Rev. D **90**, 072001 (2014).

[15] V.M. Abazov *et al.* (D0 Collaboration), Measurement of the asymmetry in angular distributions of leptons produced in dilepton $t\bar{t}$ final states in $p\bar{p}$ collisions at $\sqrt{s} = 1.96$ TeV, Phys. Rev. D **88**, 112002 (2013).